A&A 603, A7 (2017)
DOI: 10.1051/0004-6361/201630212

Astronomy & Astrophysics

Energy distribution of relativistic electrons in the young supernova remnant G1.9+0.3

Felix Aharonian[1,2,3], Xiao-na Sun[2], and Rui-zhi Yang[2]

[1] Dublin Institute for Advanced Studies, 31 Fitzwilliam Place, Dublin 2, Ireland
[2] Max-Planck-Institut für Kernphysik, PO Box 103980, 69029 Heidelberg, Germany
e-mail: ryang@mpi-hd.mpg.de
[3] MEPHI, Kashirskoe shosse 31, 115409 Moscow, Russia

Received 7 December 2016 / Accepted 20 April 2017

ABSTRACT

The broad-band X-ray observations of the youngest known galactic supernova remnant (SNR), G1.9+0.3, provide unique information about the particle acceleration at the early stages of evolution of supernova remnants. Based on the publicly available X-ray data obtained with the *Chandra* and *NuSTAR* satellites over two decades in energy, we derived the energy distribution of relativistic electrons under the assumption that detected X-rays are of entirely synchrotron origin. The acceleration of electrons was found to be an order of magnitude slower than the maximum rate provided by the shock acceleration in the nominal Bohm diffusion regime. We discuss the implications of this result in the context of contribution of SNRs to the Galactic Cosmic Rays at PeV energies.

Key words. supernovae: individual: SNR G1.9+0.3 – gamma rays: ISM

1. Introduction

Supernova remnants (SNRs) are believed to be the sites where the bulk of Galactic cosmic rays (CRs) are accelerated up to PeV energies (1 PeV = 10^{15} eV) (see, e.g., Hillas 2013; Blasi 2013). In recent years, significant progress has been achieved in a few directions of exploring the CR acceleration in SNRs, in particular using the γ-ray observations in the MeV/GeV and TeV energy bands (see, e.g., Aharonian 2013). In particular, the detection of the so-called π^0-decay bump in the spectra of several mid-age SNRs, is considered as a substantial evidence of acceleration of protons and nuclei in SNRs. Moreover, the detection of more than ten young (a few thousand years old or younger) SNRs in TeV γ-rays highlights these objects as efficient particle accelerators, although the very origin of γ-rays (leptonic or hadronic?) is not yet firmly established. More disappointingly, so far all TeV emitting SNRs do not show energy spectra that would continue as a hard power-law beyond 10 TeV. For a hadronic origin of detected γ-rays, the "early" cutoffs in the energy spectra of γ-rays around or below 10 TeV imply a lack of protons inside the shells of SNRs with energies significantly larger than 100 TeV, and, consequently, SNRs do not operate as PeVatrons. However, there are two possibilities that would allow us to avoid such a dramatic conclusion for the current paradigm of Galactic CRs:

(i) The detected TeV gamma-rays are of leptonic (inverse Compton) origin. Of course, alongside the relativistic electrons, protons and nuclei can (should) be accelerated as well, but we do not see the related γ-radiation because of their ineffective interactions caused by the low density of ambient gas;

(ii) SNRs do accelerate protons to PeV energies, however it occurs at early stages of evolution of SNRs when the shock speeds exceed 10 000 km s^{-1}; we do not see the corresponding radiation well above 10 TeV because the PeV protons have already left the remnant.

Both these scenarios significantly limit the potential of gamma-ray observations for the search for CR PeVatrons. Fortunately, there is another radiation component, which contains independent and complementary information about these extreme accelerators. It is related to the synchrotron radiation of accelerated electrons, namely to the shape of the energy spectrum of radiation in the cutoff region which can serve as a distinct signature of the acceleration mechanism and its efficiency. In the shock acceleration scheme, the maximum energy of accelerated particles, $E_0 \propto B\, v_{\rm sh}^2$. Therefore, the epoch of the first several hundred years of evolution of a SNR, when the shock speed $v_{\rm sh}$ exceeds 10 000 km s^{-1} and the magnetic field is large ($B \gg 10\ \mu$G) could be an adequate stage for operation of a SNR as a PeVatron, provided, of course, that the shock acceleration proceeds close to the Bohm diffusion limit (see, e.g., Malkov & Drury 2001). Remarkably, in this regime, the cutoff energy in the synchrotron radiation of the shock-accelerated electrons is determined by a single parameter, $v_{\rm sh}^2$ (Aharonian & Atoyan 1999; Zirakashvili & Aharonian 2007). Therefore, for the known shock speed, the position of the cutoff contains an unambiguous information about the acceleration efficiency. For $v_{\rm sh} \simeq 10\,000$ km s^{-1}, the synchrotron cutoff in the spectral energy distribution (SED) is expected around 10 keV. Thus, the study of synchrotron radiation in the hard X-ray band can shed light on the acceleration efficiency of electrons, and, consequently, provide an answer as to whether or not these objects can operate as CR PeVatrons, given that in the shock acceleration scheme the acceleration of electrons and protons is expected to be identical. In this regard, G1.9+0.3, the youngest known SNR in our Galaxy (Reynolds et al. 2008; Green et al. 2008), is a perfect object to explore this unique tool.

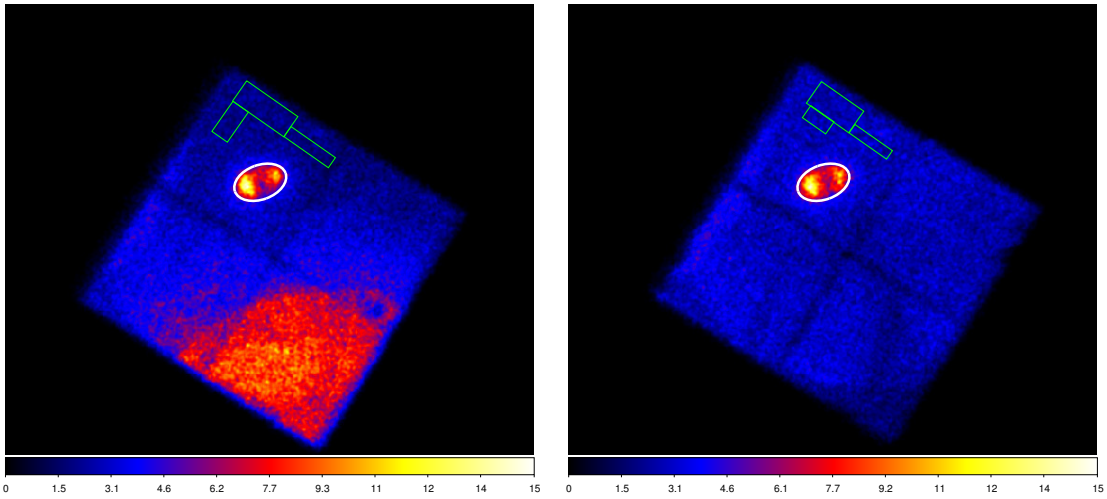

Fig. 1. Images from the observation 40001015007 for the FPMA (*left*) and FPMB (*right*) modules. The source and background regions are indicated by the white and green contours, respectively.

The X-ray observations with the *Chandra* and *NuSTAR* satellites (Reynolds et al. 2009; Zoglauer et al. 2015) cover a rather broad energy interval which is crucial for the study of the spectral shape of synchrotron radiation, in particular in the cutoff region. Such a study has been conducted by the team of the *NuSTAR* collaboration (Zoglauer et al. 2015).

In this paper we present the results of our own analysis of the *NuSTAR* and *Chandra* data with an emphasis on the study of the SED of X-ray radiation over two decades, from 0.3 keV to 30 keV. Using the synchrotron emissivity of relativistic electrons and the Markov chain Monte Carlo (MCMC) technique, we derive the energy distribution of electrons responsible for X-rays and discuss the astrophysical implications of the obtained results.

2. X-ray observations

The recent hard X-ray observations of G1.9+0.3 by the *NuSTAR* satellite are uniquely useful for understanding the acceleration and radiation processes of ultrarelativistic electrons in SNRs at the early stages of their evolution. Detailed study of the *NuSTAR* data, combined with the *Chandra* observations at lower energies, has been comprehensively carried out by Zoglauer et al. (2015). In particular, it was found that the source can be resolved into two bright limbs with similar spectral features. The combined *Chandra* and *NuSTAR* datasets have been claimed to be best described by the so-called *srcut* model (Reynolds 2008) or by the power-law function with an exponential cutoff. The characteristic cutoff energies in these two fits have been found around 3 keV and 15 keV, respectively (Zoglauer et al. 2015).

To further investigate the features of the X-ray spectrum in the cutoff region we performed an independent study based on the publicly available *Chandra* and *NuSTAR* X-ray data. For *NuSTAR*, we used the set of three observations with ID 40001015003, 40001015005, and 40001015007, including both the focal plane A (FPMA) and B (FPMB) modules. The data have been analysed using the HEASoft version 6.16, which includes NuSTARDAS, the *NuSTAR* Data Analysis Software package (the version 1.7.1 with the *NuSTAR* CALDB version 20150123). For the *Chandra* data, we used the ACIS observations with ID 12691, 12692 and 12694. The *Chandra* data reduction was performed using version 4.7 of the *Chandra* Interactive Analysis of Observations (CIAO) package.

In Fig. 1 we show the X-ray sky map above 3 keV based on the *NuSTAR* 40001015007 data set. In order to benefit from the maximum possible statistics, for the spectral analysis we have chosen the entire remnant . The background regions were selected in a way to minimise the contamination caused by the PSF wings as well as from the stray light. The excess in the south of the FPMA image is the stray light from X-rays that hit the detector without impinging on the optics (Wik et al. 2014). We use the same source regions for *Chandra* observations.

The results of our study of the spatial distribution of X-rays appeared quite similar to those reported by (Zoglauer et al. 2015). Therefore, in this paper we do not discuss the morphology of the source but focus on the study of spectral features of radiation.

The spectral shape of synchrotron radiation in the cutoff region is sensitive to the spectrum of highest energy electrons which, in turn, depends on the electron acceleration and energy loss rates. To explore a broad class of spectra, we describe the spectrum of X-rays in the following general form:

$$\frac{\mathrm{d}N}{\mathrm{d}\epsilon} = AE^{-\Gamma}\exp\left[-(\epsilon/\epsilon_0)^{\beta}\right]. \quad (1)$$

The change of the index β in the second (exponential) term allows a broad range of spectral behaviour in the cutoff region. For example, $\beta = 0$ implies a pure power-law distribution, while $\beta = 1$ corresponds to a power-law with a simple exponential cutoff.

In the fitting procedure, in addition to the three parameters ϵ_0, Γ, and β, one should introduce one more parameter, the column density $N_{\rm H}$, which takes into account the energy-dependent absorption of X-rays. We fix this parameter to the value found by Zoglauer et al. (2015) from the fit of data by their *srcut* spectral model . Strictly speaking, the best fit value of the column density should be different for different spectral models. To check the impact of different spectral models on the column density, we adopted different functions leaving the column density as a free parameter in the fitting procedure. We found that the difference of the best fit column density and the above fiducial value is less than several percent. Therefore, in order to keep the procedure simple and minimise the number of free parameters, we adopt

Table 1. Spectral fitting results for G1.9+0.3.

Model	PL index	Cutoff (keV)	β	χ^2/d.o.f.
PL	2.54 (2.52–2.56)			1089.4/666
PL+ecut	2.04 (1.98–2.10)	11.8 (10.5–13.3)		697.7/665
PL+ecut (β = 0.5)	1.65 (1.60–1.70)	1.68 (1.50–1.90)	0.5	686.2/665
PL+ecut (β = 0.33)	1.18(1.10–1.26)	0.07 (0.06–0.08)	0.33	687.5/665
PL+ecut (β free)	1.62(1.48–1.75)	1.41 (1.30–1.55)	0.48 (0.40-0.56)	685.8/664

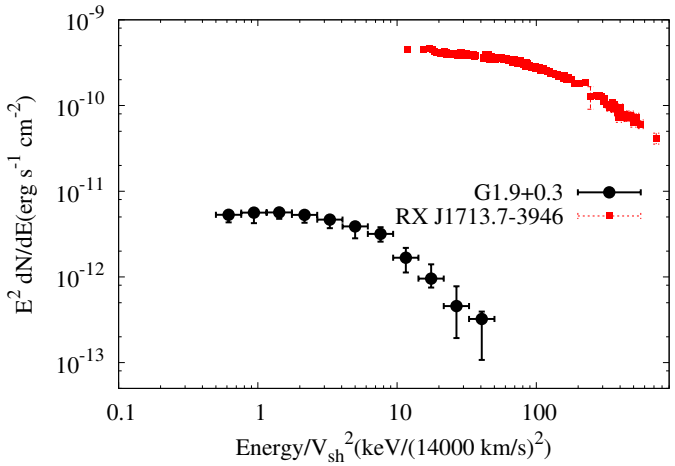

Fig. 2. Spectral points of G1.9+0.3 (this work; black circles) and RX J1713.4-3946 (red square) from Tanaka et al. (2008). The energies of the points of RX J1713.4-3946 are rescaled by the factor of the square of the ratio of shock speeds of J1713.4-3946 and G1.9+0.3: (14 000 km s^{-1}/4000 km s^{-1})^2 = 12.25.

the value $N_{\rm H} = 7.23 \times 10^{22}$ from the paper of Zoglauer et al. (2015).

The results of our fit of the *NuSTAR* and *Chandra* spectral points using the model "power-law with exponential cutoff" in the general form of Eq. (1), that is, leaving β, Γ, and ϵ as free parameters, are shown in Table 1. One can see that the best fit gives a rather narrow range of the index β around 1/2. In Table 1 we also separately show the results of the fits with three fixed values of β: 0, 1/2, and 1. While the pure-power-law spectrum ($\beta = 0$) can be unambiguously excluded, the model of power-law with a simple exponential cutoff ($\beta = 1$) is not favourable either. It is excluded at the 3σ statistical significance level. In summary, the combined *Chandra* and *NuSTAR* data are best described by the index $\beta \approx 0.5$ and $\epsilon_0 \approx 1.5$ keV.

Whereas $\beta = 1/2$ seems to be a natural outcome (see below), the cutoff energy around 1.5 keV is a rather unexpected result. Namely, it implies that the acceleration of electrons in G1.9+0.3 proceeds significantly slower than one would anticipate given the very large, 14 000 km s^{-1} shock speed (Borkowski et al. 2010). This can be seen from the comparison of the SED of G1.9+0.3 with one of the most effective particle accelerators in our Galaxy, ≈1600 yr old SNR RX J1713.4-3946 (see Fig. 2). The cutoff energy in the synchrotron spectrum of shock-accelerated electrons is proportional to the square of shock speed $v_{\rm sh}^2$ (Aharonian & Atoyan 1999). Therefore, in order to exclude the difference in the cutoff energies caused by the difference in the shock speeds, we rescale the energies of the spectral points of RX J1713.4-3946 by the factor ($v_{\rm sh}$/14 000 km s^{-1})^2, where the shock speed of RX J1713.4-3946 is about $v_{\rm sh} \simeq 4000$ km s^{-1} (Uchiyama et al. 2007). After such a normalisation, the cutoff energy of RX J1713.4-3946 becomes an order of magnitude higher than the cutoff in G1.9+0.3. The acceleration of electrons in RX J1713.4-3946 proceeds close to the Bohm diffusion limit thus providing an acceleration rate close to the maximum value(Uchiyama et al. 2007; Zirakashvili & Aharonian 2010). Consequently, we may conclude that the current acceleration rate of electrons in G1.9+0.3 is lower, by an order of magnitude, compared to the maximum possible rate.

It should be noted that the physical meaning of Eq. (1) should not be overestimated. Namely, it should be considered as a convenient analytical presentation of the given set of measured spectral points. Consequently, $\Gamma, \beta, \epsilon_0$ that enter into Eq. (1) should be treated as a combination of formal fit parameters rather than physical quantities. For example, ϵ_0 in the exponential term of Eq. (1) should not necessarily coincide with the cutoff energy (or maximum in the SED). Indeed, in different (Γ, β, ϵ_0) combinations describing the same spectral points, the parameter ϵ_0 could have significantly different values. Analogously, Γ should not be treated as a power-law index but rather a parameter which, in combination with Γ and β, determines the slope (the tangential) of the spectrum immediately before the cutoff region.

The maximum acceleration rate of particles is achieved when it proceeds in the Bohm diffusion limit. In the energy-loss-dominated regime, the spectra of synchrotron radiation can be expressed by simple analytical formulae (Zirakashvili & Aharonian 2007). Because of compression of the magnetic field, the overall synchrotron flux of the remnant is dominated by the radiation from the downstream region (see Fig. 3). The SED of the latter can be presented in the following form (Zirakashvili & Aharonian 2007)

$$\epsilon^2 \frac{{\rm d}N}{{\rm d}\epsilon} \propto \epsilon^2 (\epsilon/\epsilon_0)^{-1} \left[1 + 0.38(\epsilon/\epsilon_0)^{0.5}\right]^{11/4} \exp\left[-(\epsilon/\epsilon_0)^{1/2}\right]. \quad (2)$$

with

$$\epsilon_0 = \hbar\omega_0 = \frac{2.2\ {\rm keV}}{\eta(1+\kappa^{1/2})^2} \left(\frac{u_1}{3000\ {\rm km\ s^{-1}}}\right)^2, \quad (3)$$

where η takes into account the deviation of the diffusion coefficient from its minimum value (in the nominal Bohm diffusion limit $\eta = 1$). In the standard shock acceleration theory, the momentum index of accelerated electrons $\gamma_{\rm s} = 4$, and the ratio of the upstream and downstream magnetic fields, $\kappa = 1/\sqrt{11}$.

In Fig. 3 the spectral points of G1.9+0.3 are compared with the theoretical predictions for synchrotron radiation in the upstream and downstream regions (Zirakashvili & Aharonian 2007). The calculations are performed for two values of the parameter η characterising the acceleration efficiency: $\eta = 1$ (Bohm diffusion regime) and 20 times slower ($\eta = 20$). The good (better than 20%) agreement of the spectral points with the theoretical curves for $\eta = 20$ tells us that in G1.9+0.3 electrons are accelerated only at the 5% efficiency level.

Although in the paper of Zoglauer et al. (2015) the spectral points are not explicitly presented, thus the direct comparison with our results is not possible, the conclusions based on our

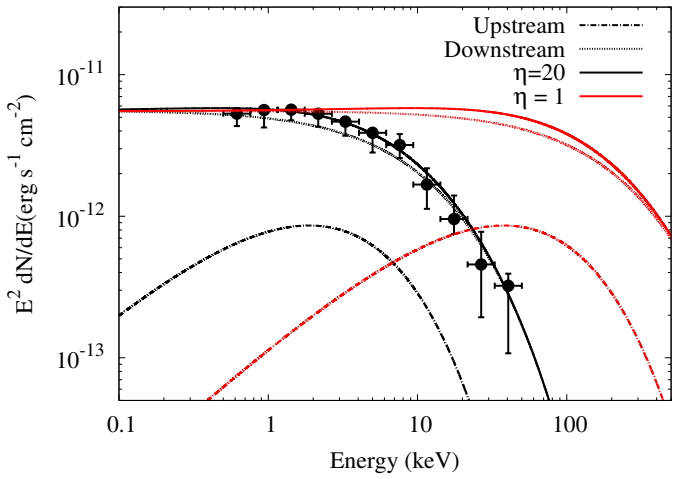

Fig. 3. The spectral points of G1.9+0.3 (this work) compared to the predictions of synchrotron radiation of the shock accelerated electrons in the downstream and upstream regions (Zirakashvili & Aharonian 2007). The calculations correspond to two regimes of diffusion: (1) Bohm diffusion, $\eta = 1$ and (2) 20 times faster diffusion, that is, $\eta = 20$.

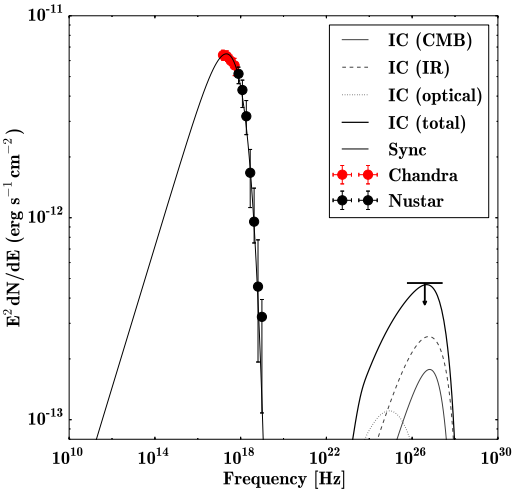

Fig. 4. X-ray SED as well as the VHE upper limit from H.E.S.S. Collaboration et al. (2014). The curves are the synchrotron and IC emissions fitted to derive the lower limit of the magnetic field.

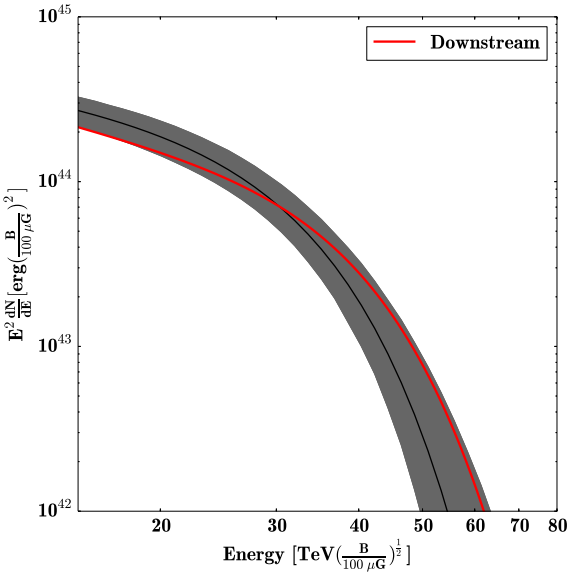

Fig. 5. Electron spectrum from the X-ray data points (black curve and shaded area) and theoreticallly predicted integrated electron spectrum in a young SNR (red curve) assuming a fast diffusion with $\eta = 20$. Also shown is the contribution from the downstream region.

study of the X-ray spectrum of G1.9+0.3 seems to be in agreement with their results.

3. Relativistic electrons and magnetic fields

The joint treatment of X-ray and γ-ray data, under the simplified assumption that the same electron population is responsible for the broad-band radiation through the synchrotron and inverse Compton channels, provides information about the magnetic field and the total energy budget in relativistic electrons. G1.9+0.3 has been observed in VHE γ-ray band with the HESS. Cherenkov telescope system. Although no positive signal has been detected (H.E.S.S. Collaboration et al. 2014), the γ-ray flux upper limits allow meaningful constraints on the average magnetic field in the X-ray and γ-ray production region. For calculations of the broad-band SED, we adopt the same background radiation fields used in H.E.S.S. Collaboration et al. (2014): the infrared component with a temperature of 48 K and energy density of 1.5 eVcm^{-3}, and the optical component with a temperature of 4300 K and the energy density of 14.6 eV cm^{-3}. The comparison of model calculations with observations (see Fig. 4) gives a lower limit of the magnetic field, $B \geq 17\ \mu$G.

Under certain assumptions, the magnetic field can be constrained also based only on the X-ray data. In the "standard" shock acceleration scenario, electrons are accelerated with the power-law index $\alpha = 2$. However because of the short radiative cooling time, their spectrum of highest energy electrons (the X-ray producers) becomes steeper, $\alpha = 2 \rightarrow 3$. Consequently, in the downstream region, where the bulk of the synchrotron radiation is produced, X-rays have a photon index $\Gamma = 2$. The synchrotron cooling time can be expressed through the magnetic field and the X-ray photon energy: $t_{\rm synch} \simeq 50(B/100\ \mu{\rm G})^{-3/2}(\epsilon/1\ {\rm keV})^{-1/2}$ years. Thus for $\epsilon \sim 1$ keV and the age of the $SNR \sim 150$ yr, we find that the magnetic field should be larger than 50 μG.

The combined *Chandra* and *NuSTAR* data cover two decades in energy, from sub-keV to tens of keV. This allows derivation of the energy distribution of electrons, $W(E) = E^2 {\rm d}N_{\rm e}/{\rm d}E$ in the most interesting region around the cutoff. The results shown in Fig. 5 are obtained using the Markov Chain Monte Carlo (MCMC) code *Naima* developed by V. Zabalza[1]. It is assumed that the magnetic field is homogeneous both in space and time. The results shown in Fig. 5 are calculated for the fiducial value of the magnetic field $B = 100\ \mu$G, however they can be rescaled for any other value of the field. We note that while the shape of the spectrum does not depend on the strength of the magnetic field, the energies of individual electrons scale as $E \propto B^{-1/2}$, and the total energy contained in electrons scales as $\propto B^{-2}$. Since in the "standard" diffusive shock acceleration (DSA) scenario the synchrotron X-ray flux is contributed mainly by the downstream region, the results in Fig. 5 are relevant to the energy distribution of electrons from the same region. For comparison, the energy distribution of electrons calculated using the formalism of Zirakashvili & Aharonian (2007) is shown.

[1] https://github.com/zblz/naima

4. Conclusions

SNRs are believed to be the major contributors to the Galactic CRs. The recent detections of TeV emission from more than ten young SNRs (of the age of a few thousand years or younger), demonstrates the ability of these objects to accelerate particles, electrons and/or protons, to energies up to 100 TeV. Yet, we do not have observational evidence of the extension of hard γ-ray spectra well beyond 10 TeV. Therefore one cannot claim an acceleration of protons and nuclei by SNRs to PeV energies. On the other hand, one cannot claim the opposite either, given the possibility that the acceleration of PeV protons and nuclei could happen at the early stages of evolution of SNRs when the shock speeds exceed 10 000 km s^{-1}. Indeed, the theoretical studies of recent years show that the best candidates for accelerators operating as PeVatrons are very young (less than 100 yrs old) supernova remnants in dense environments (see e.g. Schure & Bell 2013). Then, the escape of the highest energy particles at later stages of evolution of SNRs can explain the spectral steepening of gamma-ray spectra at multi-TeV energies from ≥1 thousand year old remnants.

In this regard, the youngest known SNR in our Galaxy, G1.9+0.3, with a measured shock speed of 14 000 km s^{-1}, seems to be a unique object in our Galaxy to explore the potential of SNRs for acceleration of protons and nuclei to PeV energies. Such measurements have been performed with the HESS array of Cherenkov telescopes. Unfortunately, no positive signal has been detected. On the other hand, the recent observations of G1.9+0.3 in hard X-rays by *NuSTAR* provide unique information about the acceleration efficiency of electrons. Together with *Chandra* data at lower energies, these data allow model-independent conclusions. Although the general shape of the energy spectrum of X-rays is in very good agreement with predications of the diffusive shock-acceleration theory, the acceleration rate appears an order of magnitude slower relative to the maximum acceleration rate achieved in the nominal Bohm diffusion limit.

It should be noted that the deviation from the Bohm diffusion concerns not only the larger absolute value of the diffusion coefficient, but also the energy dependence of the latter. The diffusion coefficient written in the conventional form $D(E) \propto E^{\lambda}$, allows consideration of diffusion in a broad range of acceleration regimes. Then, in the synchrotron-loss-dominated regime, the energy distribution of electrons in the cutoff region has an exponential form, $N(E) \propto \exp[-(E/E_0)^{\beta_e}]$ with $\beta_e = \lambda + 1$ (see Eq. (19) from Zirakashvili & Aharonian (2007)). Correspondingly, the index β characterising the spectrum of synchrotron radiation in the cutoff region, is $\beta = (1+\lambda)/(3+\lambda)$. In particular, the values of $\lambda = 0$, 1/3, and 1, which correspond to the energy-independent, Kolmogorov, and Bohm diffusion regimes, give $\beta = 1/3$, 2/5, and 1/2, respectively. We note that the energy-independent diffusion in the synchrotron-loss-dominated regime results in an X-ray spectrum similar to the one formed in the case of the Bohm diffusion but in the age-limited regime. However, strictly speaking, because of the escape, the electrons in the age-limited regime of acceleration might have a steeper spectrum[2], that is, $\beta_e \geq 1$. Although the results of the current analysis give a preference to the interval of $\beta = 0.4$–0.56, the value of 1/3 cannot be excluded (see Table 1).

To a certain extent, the relatively low acceleration rate of electrons in G1.9+0.3, in terms of the nominal rate of acceleration in the Bohm diffusion limit (for the given speed of the shock), is a surprise outcome, especially when compared with SNRs in which the acceleration of electrons proceeds in the regime close to the Bohm diffusion. For comparison, the detailed modelling of young SNRs Cas A (Zirakashvili et al. 2014) and RX J1713.4-3946 (Zirakashvili & Aharonian 2010), shows that the η parameter characterising the acceleration efficiency cannot significantly deviate from $\eta = 1$. If the acceleration of protons and nuclei proceeds in the same manner as the electron acceleration, this result would imply inability of G1.9+0.3 to operate as a PeVatron. Apparently, the observations of G1.9+0.3 alone are not sufficient to decide whether or not this conclusion can be generalised for other SNRs.

Acknowledgements. The authors appreciate the constructive and very helpful comments and suggestions of the anonymous referees.

References

Aharonian, F. A. 2013, Astropart. Phys., 43, 71
Aharonian, F. A. & Atoyan, A. M. 1999, A&A, 351, 330
Blasi, P. 2013, A&ARv, 21, 70
Borkowski, K. J., Reynolds, S. P., Green, D. A., et al. 2010, ApJ, 724, L161
Fritz, K. D. 1989, A&A, 214, 14
Green, D. A., Reynolds, S. P., Borkowski, K. J., et al. 2008, MNRAS, 387, L54
H.E.S.S. Collaboration, Abramowski, A., Aharonian, F., et al. 2014, MNRAS, 441, 790
Hillas, A. M. 2013, Astropart. Phys., 43, 19
Malkov, M. A., & Drury, L. O. 2001, Rep. Progr. Phys., 64, 429
Reynolds, S. P. 2008, ARA&A, 46, 89
Reynolds, S. P., Borkowski, K. J., Green, D. A., et al. 2008, ApJ, 680, L41
Reynolds, S. P., Borkowski, K. J., Green, D. A., et al. 2009, ApJ, 695, L149
Schure, K. M., & Bell, A. R. 2013, MNRAS, 435, 1174
Tanaka, T., Uchiyama, Y., Aharonian, F. A., et al. 2008, ApJ, 685, 988
Uchiyama, Y., Aharonian, F. A., Tanaka, T., Takahashi, T., & Maeda, Y. 2007, Nature, 449, 576
Wik, D. R., Hornstrup, A., Molendi, S., et al. 2014, ApJ, 792, 48
Zirakashvili, V. N., & Aharonian, F. 2007, A&A, 465, 695
Zirakashvili, V. N., & Aharonian, F. A. 2010, ApJ, 708, 965
Zirakashvili, V. N., Aharonian, F. A., Yang, R., Oña-Wilhelmi, E., & Tuffs, R. J. 2014, ApJ, 785, 130
Zoglauer, A., Reynolds, S. P., An, H., et al. 2015, ApJ, 798, 98

[2] This statement is correct for the epochs when the electrons start to escape the shell. The case of formation of the electron spectrum in the age-limited regime at the presence of particle escape has not been yet quantitatively explored in the literature. However, since the probability of the electron escape increases with energy, it is clear that the escape should make the spectrum of particles inside the accelerator steeper.

Appendix A

The cutoff region in the distribution of parent electrons $F(E)$ has a shape similar to the synchrotron spectrum given by Eq. (2), $F(E) \propto \exp[-(E/E_0)^{\beta_e}]$ with the following simple relation between β_e and β (Fritz 1989):

$$\beta = \frac{\beta_e}{2+\beta_e}. \quad (A.1)$$

Thus the cutoff region in the spectrum of synchrotron radiation is much smoother than the cutoff region of the spectrum of parent electrons. For any electron distribution, the synchrotron cutoff cannot be sharper than the simple exponential decline ($\beta = 1$), which can only be witnessed in the case of an abrupt cutoff in the spectrum of parent electrons ($\beta_e \to \infty$). In the case of a simple exponential cutoff in the electron spectrum ($\beta_e = 1$), the corresponding synchrotron cutoff region is very shallow with $\beta = 1/3$. Formally, such spectra can be formed during the shock acceleration of electrons in the Bohm diffusion regime when the maximum energy of electrons is determined by the age of the source rather than by energy losses of electrons. However, in the particular case of young SNRs, when the electrons are accelerated up to 100 TeV and beyond (otherwise one cannot explain the observed X-ray data), with any reasonable set of parameters (magnetic field, age of the source, shock speed, etc.), the acceleration proceeds in the electron energy-loss regime, and the maximum energy is determined from the competition between the acceleration and energy loss rates. In this case, the spectrum of electrons exhibits a super exponential cutoff, namely $\beta_e = 2$ (Zirakashvili & Aharonian 2007). Correspondingly, the synchrotron spectrum contains, in accordance with Eq. (3), a cutoff with $\beta = 1/2$.

The δ-functional approximation gives an incorrect relation between β_e and β, namely $\beta = \beta_e/2$. For example, within this approximation, the cutoff in the spectrum of synchrotron radiation with $\beta = 1$ can be interpreted as a result of the cutoff in the electron spectrum with $\beta_e = 2$. However, in reality, such a synchrotron spectrum can be formed, in accordance with Eq. (2), in the case of an abrupt cutoff in the electron spectrum, that is, for $\beta_e \to \infty$.